

Spin-split conduction band in EuB₆ and tuning of half-metallicity with external stimuliJungho Kim,^{1,2} Wei Ku,³ Chi-Cheng Lee,^{3,4,*} D. S. Ellis,² B. K. Cho,⁵ A. H. Said,¹ Y. Shvyd'ko,¹ and Young-June Kim^{2,†}¹*Advanced Photon Source, Argonne National Laboratory, Argonne, Illinois 60439, USA*²*Department of Physics, University of Toronto, Toronto, Ontario, Canada M5S 1A7*³*Condensed Matter Physics and Materials Science Department, Brookhaven National Laboratory, Upton, New York 11973, USA*⁴*Institute of Physics, Academia Sinica, Nankang, Taipei 11529, Taiwan*⁵*Center for Frontier Materials and Department of Materials Science and Engineering, GIST, Gwangju 500-712, Korea*

(Received 6 July 2011; revised manuscript received 16 January 2013; published 2 April 2013)

We report an Eu L_3 -edge resonant inelastic x-ray scattering (RIXS) investigation of the electronic structure of EuB₆. We observe that the RIXS spectral weight around 1.1 eV increases dramatically when the system is cooled below the ferromagnetic ordering temperature and follows the magnetic order parameter. This spectral feature is attributed to the intersite excitation from the local $4f$ orbital to the spin-split $5d$ orbital on the neighboring site, illustrating the essential role of exchange splitting of the conducting electrons. Based on our density functional theory calculations and the RIXS data, EuB₆ at low temperature can be consistently described with a semimetallic electronic structure with incomplete spin polarization. We propose that half-metallicity in EuB₆ can be achieved utilizing the strong tunability of the electronic structure against gate voltage, strain, and magnetic field.

DOI: [10.1103/PhysRevB.87.155104](https://doi.org/10.1103/PhysRevB.87.155104)

PACS number(s): 75.50.Cc, 71.15.Mb, 71.20.Eh, 78.70.Ck

I. INTRODUCTION

Half-metals are characterized by fully spin-polarized charge carriers, and can be very useful for spintronic applications. One of the materials that have attracted much attention as a potential half-metal is EuB₆.¹ In EuB₆, a ferromagnetic (FM) order sets in below 15 K, as shown by neutron scattering,² magnetization,³ and specific heat⁴ measurements. Its electronic property is strongly correlated with the FM order, as indicated by the sharp drop in resistivity, the blue shift of the unscreened plasma frequency, and the colossal magnetoresistance (CMR), all occurring in the vicinity of the FM ordering temperature.^{5,6} A local density approximation (LDA) + U calculation suggested that a substantial conduction band (CB) and valence band (VB) exchange splitting could lead to a half-metallic ground state in EuB₆.¹ However, a recent Andreev reflection spectroscopy⁷ reported that only about half of the carriers are spin polarized, which indicates that the ferromagnetic EuB₆ is not half-metallic. This weak spin polarization was interpreted to suggest that only the VB is spin split due to a large spontaneous Zeeman splitting with almost no CB splitting. Indeed, an angle-resolved photoemission (ARPES) experiment has reported a splitting of the VB.⁸ The conduction band splitting cannot be ignored since the coupling of the Eu- $5d$ CB to the local $4f$ moment is an essential ingredient for the ferromagnetic ordering.¹

Resonant inelastic x-ray scattering (RIXS) is a bulk-sensitive and element-specific probe of electronic structure that can address the issue of CB spin splitting in EuB₆. Much attention has been paid to $3d$ and $5d$ transition metal L edges to uncover various momentum-dependent magnetic and orbital excitations.^{9–15} In the hard x-ray regime, earlier work focused mostly on the study of electronic excitations in $3d$ transition metal compounds such as cuprates and manganites using K -edge resonances.^{16–19} Full instrumental capability of the $3d$ transition metal K -edge RIXS can be extended to the L_3 edges of rare-earth (RE) elements straightforwardly, since they are

in the same energy range. Until now, however, applications of hard x-ray RIXS to study RE compounds have been limited to core excitations.²⁰ At RE L_3 edges, RIXS probes $5d$ states directly, enabling one to study $5d$ related excitations. In particular, the $4f$ - $5d$ transitions in RE compounds provide information about the interaction between local moments and conduction electrons. Since partially occupied $4f$ states are responsible for local magnetic moments, and delocalized $5d$ states form the conduction band, magnetic properties of these materials crucially depend on the intersite interaction of the $4f$ moments through the intra-atomic d - f exchange mediated by the conduction electrons. In addition, such an interaction between the $4f$ moments through the d - f exchange mediated by conduction electrons often leads to a diverse range of magnetic and electronic properties, such as CMR and half-metallicity.^{21–25}

In this work we report Eu L_3 -edge RIXS study of the electronic structure of EuB₆ at low temperatures. We observe a large resonant enhancement of excitations in the energy range of 1–6 eV, which shows a complex incident energy dependence. When the incident photon energy is fixed at $E_i = 6982$ eV, we could selectively enhance low energy excitations below 2 eV, which correspond to transitions from the local $4f$ orbitals to the spin-split $5d$ orbitals on the neighboring sites. This low energy RIXS spectral weight grows significantly as the sample is cooled below the FM transition temperature, closely mimicking the temperature dependence of the ordered magnetic moment. This observation suggests that the FM ordering is accompanied by a fairly substantial exchange splitting of the conduction band, which opens up the $4f$ - $5d$ transition channel. Our density functional theory calculations combined with the RIXS findings point to a slightly doped semimetallic system with incomplete spin polarization. This provides a natural way to explain the previously reported Andreev reflection data.⁷ We also show that such a system can be driven into a desired half-metallic state via gate voltage, strain, or magnetic field.

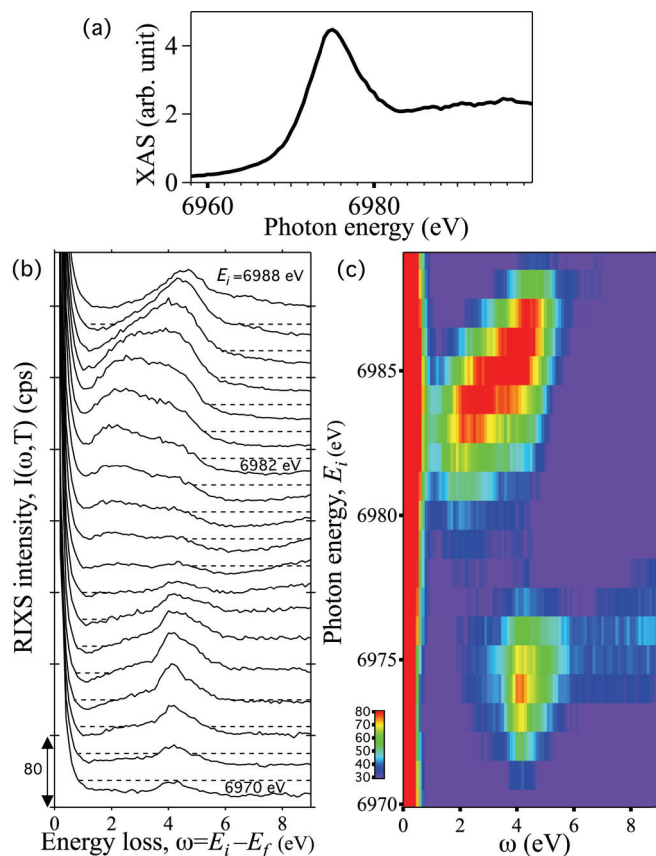


FIG. 1. (Color online) (a) The Eu L_3 -edge XAS spectrum measured in the partial fluorescence yield. (b) and (c) Incident photon energy dependence of RIXS intensity as a function of energy loss ω and incident photon energies $6970 \leq E_i \leq 6988$ eV.

II. EXPERIMENT

The Eu L_3 -edge RIXS measurements were performed using the MERIX spectrometer at the 30ID beamline of the Advanced Photon Source (APS).²⁶ The single-crystal sample was synthesized by a boro-thermal method as described in detail elsewhere.²⁷ The sample is mounted in a closed-cycle He cryostat. Throughout the RIXS measurements, sample temperature was controlled within 0.2 K of stability. The total energy resolution of the MERIX spectrometer at the Eu L_3 edge is 140 meV, determined by the full-width-half-maximum (FWHM) of the elastic scattering peak. This is achieved using a 1 m Ge(620) spherical, diced analyzer, and a position-sensitive microstrip detector.²⁸ The RIXS data were normalized by the photon flux and no additional scaling of the data was done. The incident photon polarization component was perpendicular to the scattering plane (σ polarization).

III. RESULTS

Figure 1(a) shows the Eu L_3 x-ray absorption spectrum (XAS) which was collected in the partial fluorescence yield mode. The XAS spectrum exhibits a single dipolar transition peak at 6975 eV, confirming divalent Eu in EuB₆. Figures 1(b) and 1(c) show RIXS spectra and 2D color plot of RIXS intensities, respectively, measured at room temperature and at the momentum transfer of $\mathbf{Q} = (1.5, 0, 0)$ with the incident

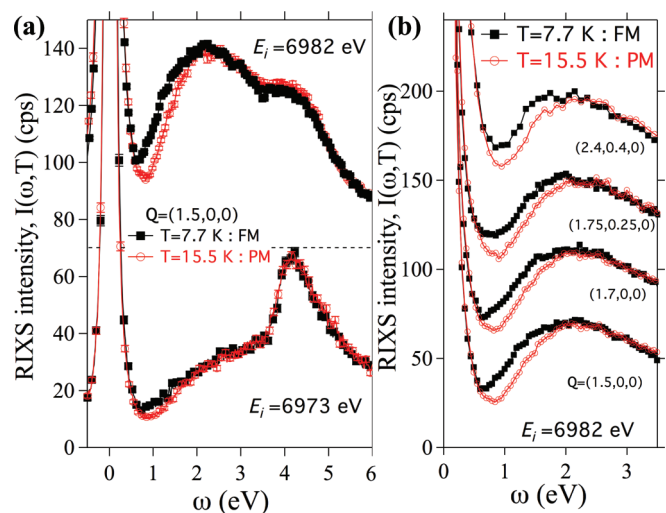


FIG. 2. (Color online) (a) Comparison of the RIXS spectra in the FM phase ($T = 7.7$ K) and the PM phase ($T = 15.5$ K) for two selected incident photon energies ($E_i = 6973$ and 6982 eV) at $\mathbf{Q} = (1.5, 0, 0)$. Low energy excitations below 2 eV are largely enhanced at $E_i = 6982$ eV. (b) RIXS spectra for a number of different \mathbf{Q} positions measured with $E_i = 6982$ eV.

photon energy (E_i) changing from 6970 to 6988 eV.²⁹ Each spectrum is measured by scanning the scattered photon energy E_f with E_i fixed, and plotted as a function of the energy loss $\omega \equiv E_i - E_f$. The RIXS spectra in Fig. 1(b) are shifted vertically for clarity. The zero intensity level for each spectrum is shown by a broken line. A strong elastic signal is observed at $\omega = 0$ for all spectra. A constant energy loss (Raman-like) feature at $\omega \approx 4$ eV resonates at $6972 \leq E_i \leq 6977$ eV, which belongs to the main peak energy range in the XAS spectrum. A broad spectral feature between 0.5 and 5 eV is also observed to resonate at $6982 \leq E_i \leq 6988$ eV. In the latter case, additional XAS final states seem to exist at this higher energy hidden in the broad, featureless intensity and we can pick out these additional intermediate states from the RIXS spectra. This feature cannot be a valence fluorescence because both incident and scattered photon energy is well above (~ 10 eV) the so-called white line absorption energy (6975 eV).³⁰ The E_i dependence of this broad feature is reminiscent of that observed in a number of K -edge RIXS studies on cuprates.^{31–34} The spectral features are only observed within a particular range of incident energies. The signal of the lower energy excitation is enhanced for $E_i = 6982$ eV. As E_i increases, a higher energy signal is gradually enhanced and eventually disappears above $E_i = 6988$ eV. This observation suggests that this spectral feature arises from “shake-up” excitations of electron-hole pairs, as described in Ref. 9.

We have measured RIXS spectra below ($T = 7.7$ K) and above ($T = 15.5$ K) the FM ordering temperature for $6970 \leq E_i \leq 6988$ eV at $\mathbf{Q} = (1.5, 0, 0)$. Figure 2(a) shows such RIXS spectra for the selected incident photon energies ($E_i = 6973$ and 6982 eV). Clearly the RIXS intensity in the FM phase in the 0.5–2 eV region is significantly greater than that in the PM phase, especially for $E_i = 6982$ eV. Note that the increase in the 0.5–2 eV region cannot be due to a shift since the spectra overlap both below and above this frequency

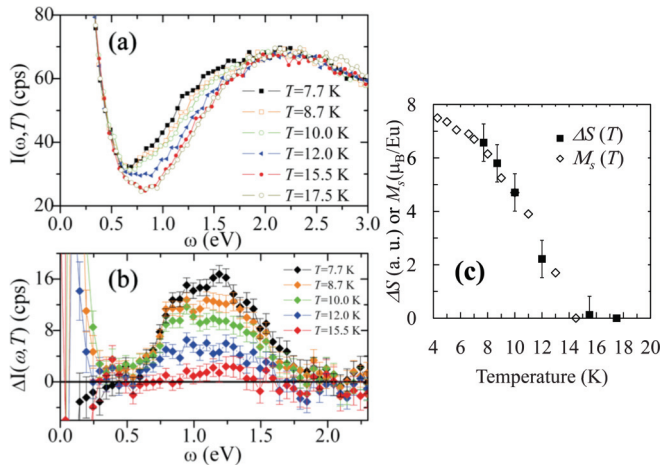


FIG. 3. (Color online) (a) RIXS spectra for $E_i = 6982$ eV at various temperatures from above to below $T_{c1} = 15$ K. The RIXS intensity below 2 eV grows systematically as T decreases below T_{c1} . (b) The difference between the FM phase and the PM phase $\Delta I(\omega, T) = I(\omega, T) - I(\omega, 17.5 \text{ K})$. (c) Filled squares: the RIXS integrated intensity change $\Delta S(T) \equiv \int \Delta I(\omega, T) d\omega$ ($0.5 \leq \omega \leq 2$ eV). Open diamonds: Spontaneous magnetic moment per Eu atom obtained from the Arrott plot analysis of the magnetization data (from Ref. 4).

region. The quasielastic background, which usually varies with temperature, stays the same, since actual temperature change is quite small. We focus on the temperature and momentum dependence of the RIXS spectra for $E_i = 6982$ eV in this work. We have also measured RIXS spectra for a number of different Q positions. Figure 2(b) shows that the increase in the 0.5–2 eV region exhibits little momentum dependence.

Detailed temperature dependence of the RIXS spectra below and above the FM transition are plotted in Fig. 3(a). In order to show the temperature dependence more clearly, we plot the difference spectra between the FM phase and the PM phase in Fig. 3(b), in which the spectrum obtained at $T = 17.5$ K represents the PM phase. As temperature is lowered, RIXS intensity grows gradually without changing its energy position. In Fig. 3(c) the integrated RIXS intensity from Fig. 3(b) is compared to the temperature dependence of the spontaneous magnetic moment from Ref. 4, which represents magnetic order parameter. The close similarity between the two indicates that the RIXS spectral weight increase upon entering the FM phase is intimately related to the FM order parameter. Such a strong temperature dependence of the RIXS spectra has not been observed before since RIXS typically measures in the energy range much higher than thermal energy. Our observation is reminiscent of the case in manganites,¹⁸ for which the spectral weight of the intersite d - d excitation was found to be sensitive to the magnetic ground state, but quantitative comparison of the magnetization and the RIXS intensity was not possible.

To guide a theoretical analysis of our excitation spectra and understand the ground state electronic structure, we performed a first-principles calculation by an all-electron full-potential method using linearized augmented plane wave basis within the LDA + U approximation ($U = 7$ eV on Eu f orbital) implemented by Wien2k code.³⁵ To remove the well-known self-interaction problem of the approximate energy functional,

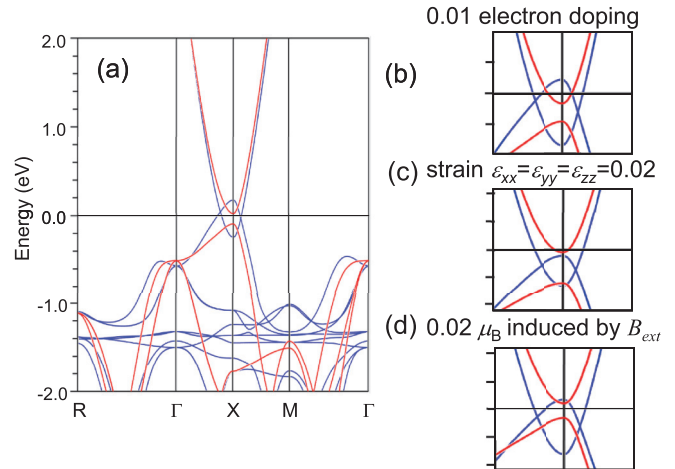


FIG. 4. (Color online) (a) LDA + U band structure of EuB_6 with 0.5 eV self-interaction correction. The metallic spin-majority and gapped spin-minority bands are colored blue and red, respectively. (b) Band structures near the X point under 0.01 electron doping per formula unit. This represents the realistic band structure of our sample at low temperatures. Applied gate voltage could drive the system into the half-metallic state shown in (a). Likewise, the effects of (c) stress and (d) external magnetic field can be used to tune the electronic structure of EuB_6 . All tick marks in (a)–(d) are at every 0.2 eV step.

we apply a “real-space scissor operator” to split the energy of the occupied and unoccupied orbitals by another 0.5 eV in the low-energy effective Hamiltonian obtained from the first-principles Wannier function analysis.³⁶ This procedure, unlike the rigid band shift produced by the common “ k -space scissor operator,” allows k -dependent rehybridization of the orbitals, thus producing a different band dispersion and a set of consistent eigenorbitals. As shown in Fig. 4(a), in agreement with previous calculations,^{1,37} the band structure of EuB_6 around the Fermi level (E_F) is characterized by the occupied B- $2p$ VB, Eu- $4f$ lower Hubbard band, and the unoccupied Eu- $5d$ CB. The VB and CB approach each other in the vicinity of the X point of the Brillouin zone, while the flat $4f$ band stays about 1–2 eV below E_F .³⁸

IV. DISCUSSION

In our LDA + U calculations, the bandwidth difference of the flat $4f$ bands between the FM and PM (AFM) phases is about 0.1 eV, which is too small to explain the observed large change in the RIXS spectra. Therefore, the only relevant physical effects on the particle-hole channel by the FM ordering is the exchange splittings of $5d$ bands. In the case of optical spectra, which is most sensitive to the phase space available in the long-wavelength limit, the FM ordering dramatically influences the Drude component.⁶ This is accompanied by a small *reduction* of the spectral weight associated with the high-energy interband transition in the FM phase, as a secondary effect, likely due to the optical sum rule.³⁹ In contrast, RIXS probes mostly the short-wavelength regime, in which the intraband feature is negligible, and more localized $4f$ orbitals dominate the low energy excitation spectrum. Our observation of very little momentum dependence also indicates that the observed excitation involves relatively flat bands (e.g.,

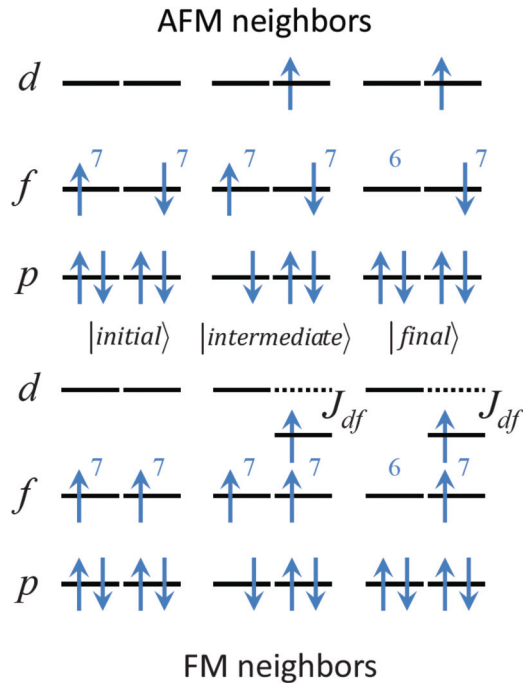


FIG. 5. (Color online) Schematics of the RIXS processes when magnetic moments on neighboring atoms are opposite (top figure) or parallel (bottom). The numbers next to the *f*-state spins indicate the number of electrons in the corresponding *f* state. J_{df} is the effective on-site *d*-*f* exchange coupling.

f bands) since excitations from wide bands tend to show strong momentum dependencies. This strong coupling to the 4*f* bands is precisely what gives RIXS the sensitivity to *f*-*d* excitation that reflects the spin splitting of the 5*d* bands.

We associate the observed RIXS excitation in the 0.5–2 eV range with an *intersite* transition from the local 4*f* orbital to the spin-split 5*d* orbital on the neighboring site. The leading RIXS process for such an intersite *d*-*f* excitation is illustrated schematically in Fig. 5. In the intermediate state, the core electron is kicked directly to the 5*d* orbital of the neighboring site. Due to the intersite nature of the process, it has a small matrix element and requires higher incident energy, but it is more sensitive to the on-site magnetic correlation.⁴⁰ The FM order-induced changes in the intersite *d*-*f* excitations arise from the effective on-site *d*-*f* exchange J_{df} . When neighbors are antiferromagnetically aligned, only the higher energy *f*-*d* transitions could occur. On the other hand, the J_{df} lowers the *f*-*d* transition energy between FM neighbors as depicted in Fig. 5. The size of J_{df} can be estimated from our LDA + *U* calculations. Since the energy difference between the spin-up and spin-down Eu 5*d* states (CB) is about 0.6 eV and there are seven *f* electrons, J_{df} is about 0.08 eV. That is, the finite

J_{df} , i.e., the spin-split CB in the FM phase could give rise to the observed temperature dependence of the RIXS spectral weight. This illustrates the importance of the spin polarization of the CB.

Our result of the exchange splitting of the CB, as well as the previous observation of 56% carrier spin polarization,⁷ can be consistently described by assuming that the system is slightly (~1%) electron doped, presumably from some (3%) B vacancies.⁴¹ As shown in Fig. 4(b), due to the efficient *d*-*f* exchange in the FM phase, the low-temperature electronic structure would be that of a semimetal with incomplete spin polarization, which is due to a electron pocket of the minority-spin conduction band. Such an electronic structure is expected to be highly tunable against external stimuli. For example, Figs. 4(a), 4(c), and 4(d) demonstrate how half-metallicity can be achieved via gate voltage, tensile strain, and external magnetic field, respectively. Changes in the minority-spin conduction band dispersion, as well as the exchange splitting, give rise to such tunability towards half-metallicity. Such a sensitive response to external stimuli makes EuB₆ an interesting potential candidate for spin-dependent transport devices, exploiting the spin-filter, giant magnetoresistance, or tunneling magnetoresistance effects.

V. SUMMARY

Our Eu *L*₃-edge resonant inelastic x-ray scattering (RIXS) experiments have revealed magnetically sensitive RIXS spectral weight, which can be understood as arising from the lowering of the intersite *f*-*d* transition energy between ferromagnetic neighbors by the effective on-site *d*-*f* exchange. Our density functional theory calculations combined with the RIXS findings suggest an incomplete spin-polarized semimetallic electronic structure for EuB₆ at low temperature. We also find that highly desirable half-metallicity can be achieved in such an electronic structure, which exhibits a strong tunability against gate voltage, strain, and magnetic field. It will be interesting to study thin films^{42,43} and nanowire/nanotube⁴⁴ of EuB₆, which provide a platform for tuning the electronic and magnetic properties via these external stimuli.

ACKNOWLEDGMENTS

Work at the University of Toronto was supported by the NSERC of Canada, Canadian Foundation for Innovation, and Ontario Ministry of Research and Innovation. Theoretical work at Brookhaven National Laboratory was supported by the U.S. DOE, Office of Basic Energy Science, under Contract No. DE-AC02-98CH10886 and DOE CMSN. Use of the Advanced Photon Source was supported by the U.S. DOE, Office of Science, under Contract No. DE-AC02-06CH11357. Work at GIST was supported by the Ministry of Education, Science and Technology of the Republic of Korea (2011-0028736).

*Current address: School of Materials Science, Japan Advanced Institute of Science and Technology (JAIST), 1-1 Asahidai, Nomi, Ishikawa 923-1292, Japan.

†Corresponding author: yjkim@physics.utoronto.ca

¹J. Kuneš and W. E. Pickett, *Phys. Rev. B* **69**, 165111 (2004).

²W. Henggeler, H.-R. Ott, D. P. Young, and Z. Fisk, *Solid State Commun.* **108**, 929 (1998).

³S. Süllow, I. Prasad, M. C. Aronson, J. L. Sarrao, Z. Fisk, D. Hristova, A. H. Lacerda, M. F. Hundley, A. Vigliante, and D. Gibbs, *Phys. Rev. B* **57**, 5860 (1998).

- ⁴S. Süllow, I. Prasad, M. C. Aronson, S. Bogdanovich, J. L. Sarrao, and Z. Fisk, *Phys. Rev. B* **62**, 11626 (2000).
- ⁵C. N. Guy, S. von Molnar, J. Etourneau, and Z. Fisk, *Solid State Commun.* **33**, 1055 (1980).
- ⁶L. Degiorgi, E. Felder, H. R. Ott, J. L. Sarrao, and Z. Fisk, *Phys. Rev. Lett.* **79**, 5134 (1997).
- ⁷X. Zhang, S. von Molnár, Z. Fisk, and P. Xiong, *Phys. Rev. Lett.* **100**, 167001 (2008).
- ⁸J. D. Denlinger *et al.*, 2007 APS March Meeting Bulletin, A7.00003.
- ⁹L. J. P. Ament, M. van Veenendaal, T. P. Devereaux, J. P. Hill, and J. van den Brink, *Rev. Mod. Phys.* **83**, 705 (2011).
- ¹⁰L. Braicovich, J. van den Brink, V. Bisogni, M. M. Sala, L. J. P. Ament, N. B. Brookes, G. M. De Luca, M. Salluzzo, T. Schmitt, V. N. Strocov, and G. Ghiringhelli, *Phys. Rev. Lett.* **104**, 077002 (2010).
- ¹¹J. Schlappa, K. Wohlfeld, K. J. Zhou, M. Mourigal, M. W. Haverkort, V. N. Strocov, L. Hozoi, C. Monney, S. Nishimoto, S. Singh, A. Revcolevschi, J.-S. Caux, L. Patthey, H. M. Rønnow, J. van den Brink, and T. Schmitt, *Nature (London)* **485**, 82 (2012).
- ¹²M. L. Tacon, G. Ghiringhelli, J. Chaloupka, M. Sala, V. Hinkov, M. Haverkort, M. Minola, M. Bakr, K. Zhou, S. Blanco-Canosa, C. Monney, Y. Song, G. Sun, C. Lin, G. D. Luca, M. Salluzzo, G. Khaliullin, T. Schmitt, L. Braicovich, and B. Keimer, *Nat. Phys.* **7**, 720 (2011).
- ¹³J. Kim, D. Casa, M. H. Upton, T. Gog, Y.-J. Kim, J. F. Mitchell, M. van Veenendaal, M. Daghofer, J. van den Brink, G. Khaliullin, and B. J. Kim, *Phys. Rev. Lett.* **108**, 177003 (2012).
- ¹⁴J. Kim, A. H. Said, D. Casa, M. H. Upton, T. Gog, M. Daghofer, G. Jackeli, J. van den Brink, G. Khaliullin, and B. J. Kim, *Phys. Rev. Lett.* **109**, 157402 (2012).
- ¹⁵X. Liu, V. M. Katukuri, L. Hozoi, W.-G. Yin, M. P. M. Dean, M. H. Upton, J. Kim, D. Casa, A. Said, T. Gog, T. F. Qi, G. Cao, A. M. Tsvelik, J. van den Brink, and J. P. Hill, *Phys. Rev. Lett.* **109**, 157401 (2012).
- ¹⁶M. Z. Hasan, E. D. Isaacs, Z.-X. Shen, L. L. Miller, K. Tsutsui, T. Tohyama, and S. Maekawa, *Science* **288**, 1811 (2000).
- ¹⁷Y. J. Kim, J. P. Hill, C. A. Burns, S. Wakimoto, R. J. Birgeneau, D. Casa, T. Gog, and C. T. Venkataraman, *Phys. Rev. Lett.* **89**, 177003 (2002).
- ¹⁸S. Grenier, J. P. Hill, V. Kiryukhin, W. Ku, Y.-J. Kim, K. J. Thomas, S.-W. Cheong, Y. Tokura, Y. Tomioka, D. Casa, and T. Gog, *Phys. Rev. Lett.* **94**, 047203 (2005).
- ¹⁹J. P. Hill, G. Blumberg, Y.-J. Kim, D. S. Ellis, S. Wakimoto, R. J. Birgeneau, S. Komiya, Y. Ando, B. Liang, R. L. Greene, D. Casa, and T. Gog, *Phys. Rev. Lett.* **100**, 097001 (2008).
- ²⁰H. Yamaoka, M. Taguchi, A. M. Vlaicu, H. Ohashi, K. Yokoi, D. Horiguchi, T. Tochio, Y. Ito, K. Kawatsura, K. Yamamoto, A. Chainani, S. Shin, M. Shiga, and H. Wada, *J. Phys. Soc. Jpn.* **75**, 034702 (2006).
- ²¹S. A. Wolf, D. D. Awschalom, R. A. Buhrman, J. M. Daughton, S. von Molnár, M. L. Roukes, A. Y. Chtchelkanova, and D. M. Treger, *Science* **294**, 1488 (2001).
- ²²J. M. D. Coey and S. Sanvito, *J. Phys. D: Appl. Phys.* **37**, 988 (2004).
- ²³R. A. de Groot, F. M. Mueller, P. G. van Engen, and K. H. J. Buschow, *Phys. Rev. Lett.* **50**, 2024 (1983).
- ²⁴M. I. Katsnelson, V. Y. Irkhin, L. Chioncel, A. I. Lichtenstein, and R. A. de Groot, *Rev. Mod. Phys.* **80**, 315 (2008).
- ²⁵A. Schmehl, V. Vaithyanathan, A. Herrnberger, S. Thiel, C. Richter, M. Liberati, T. Heeg, M. Rockerath, L. F. Kourkoutis, S. Muhlbauer, P. Boni, D. A. Muller, Y. Barash, J. Schubert, Y. Idzerda, J. Mannhart, and D. G. Schlom, *Nat. Mater.* **6**, 882 (2007).
- ²⁶Y. Shvyd'ko, J. Hill, C. Burns, D. Coburn, B. Brajuskovic, D. Casa, K. Goetze, T. Gog, R. Khachatryan, J.-H. Kim, C. Kodituwakku, M. Ramanathan, T. Roberts, A. Said, H. Sinn, D. S. d, S. Stoupin, M. Upton, M. Wiczorek, and H. Yavas (2012), [doi:10.1016/j.elspec.2012.09.003](https://doi.org/10.1016/j.elspec.2012.09.003)
- ²⁷J.-S. Rhyee, B. K. Cho, and H.-C. Ri, *Phys. Rev. B* **67**, 125102 (2003).
- ²⁸S. Huotari, G. Vanko, F. Albergamo, C. Ponchut, H. Graafsma, C. Henriquet, R. Verbeni, and G. Monaco, *J. Synch. Rad.* **12**, 467 (2005).
- ²⁹For all data presented in this paper, the self-absorption correction for E_f has been made following the approach in L. Tröger *et al.*, *Phys. Rev. B* **46**, 3283 (1992).
- ³⁰Note that a dominant valence fluorescence channel due to dipole transitions from valence Eu $5d$ electrons to $2p$ core holes does not exist in the divalent Eu of EuB_6 .
- ³¹P. Abbamonte, C. A. Burns, E. D. Isaacs, P. M. Platzman, L. L. Miller, S. W. Cheong, and M. V. Klein, *Phys. Rev. Lett.* **83**, 860 (1999).
- ³²J. Kim, D. S. Ellis, T. Gog, D. Casa, and Y.-J. Kim, *Phys. Rev. B* **81**, 073109 (2010).
- ³³L. Lu, J. N. Hancock, G. Chabot-Couture, K. Ishii, O. P. Vajk, G. Yu, J. Mizuki, D. Casa, T. Gog, and M. Greven, *Phys. Rev. B* **74**, 224509 (2006).
- ³⁴Y.-J. Kim, J. P. Hill, S. Wakimoto, R. J. Birgeneau, F. C. Chou, N. Motoyama, K. M. Kojima, S. Uchida, D. Casa, and T. Gog, *Phys. Rev. B* **76**, 155116 (2007).
- ³⁵K. Schwarz, P. Blaha, and G. Madsen, *Comput. Phys. Commun.* **147**, 71 (2002).
- ³⁶W. Ku, H. Rosner, W. E. Pickett, and R. T. Scalettar, *Phys. Rev. Lett.* **89**, 167204 (2002).
- ³⁷S. Massidda, A. Continenza, T. M. Pascale, and R. Monnier, *Z. Phys. B: Condens. Matter* **102**, 83 (1997).
- ³⁸Y. Takakuwa, S. Suzuki, and T. Sagawa, *Jpn. J. Appl. Suppl.* **17**, 284 (1978).
- ³⁹J. Kim, Y.-J. Kim, J. Kuneš, B. K. Cho, and E. J. Choi, *Phys. Rev. B* **78**, 165120 (2008).
- ⁴⁰We note that there are many other RIXS processes that are responsible for other strong spectral features at higher energies, but only magnetically sensitive processes are considered here.
- ⁴¹R. Monnier and B. Delley, *Phys. Rev. Lett.* **87**, 157204 (2001).
- ⁴²R. Bachmann, K. N. Lee, T. H. Geballe, and A. Menth, *J. Appl. Phys.* **41**, 1431 (1970).
- ⁴³L. S. Dorneles, M. Venkatesan, M. Moliner, J. G. Lunney, and J. M. D. Coey, *Appl. Phys. Lett.* **85**, 6377 (2004).
- ⁴⁴J. Xu, X. Chen, Y. Zhao, C. Zou, Q. Ding, and J. Jian, *J. Cryst. Growth* **303**, 466 (2007).